Available online at www.sciencedirect.com

ScienceDirect

International Journal of Heat and Mass Transfer 51 (2008) 3906–3912

International Journal of HEAT and MASS TRANSFER

www.elsevier.com/locate/ijhmt

Effect of a moving plate on heat transfer in a uniform heat flux vertical channel

Assunta Andreozzi [a], Nicola Bianco [a], Oronzio Manca [b], Vincenzo Naso [a,*]

[a] Dipartimento di Energetica, TErmofluidodinamica applicata e Condizionamenti ambientali, Università degli Studi di Napoli FEDERICO II, Piazzale Tecchio 80, 80125 Napoli, Italy

[b] Dipartimento di Ingegneria Aerospaziale e Meccanica, Seconda Università degli Studi di Napoli, Real Casa dell'Annunziata, Via Roma 29, 81031 Aversa (CE), Italy

Received 25 June 2007; received in revised form 5 October 2007
Available online 24 March 2008

Abstract

A numerical investigation of mixed convection in air due to the interaction between a buoyancy flow and the flow induced by a moving plate in a vertical channel is carried out. An adiabatic plate moves at a constant velocity in the mid-plane of the channel in the direction of the buoyancy force and the principal walls of the channel are heated at uniform heat flux. The effects of the channel aspect ratio, Rayleigh and Reynolds numbers are investigated and results in terms of the dimensionless channel wall and moving plate temperatures are given. Results show that the larger the channel aspect ratio, $L/(b/2)$, the stronger the effects of the moving plate. Increasing Reynolds number significantly decreases the dimensionless temperature of the channel walls. A composite correlation between Nusselt number and Reynolds and Richardson numbers is proposed in the range from natural convection to forced convection up to $Re = 1.32 \times 10^4$ and $9.86 \times 10^{-6} \leqslant Ri \leqslant 1.15 \times 10^3$, for the channel aspect ratio in the [20.3–81.2] range.

Keywords: Mixed convection; Numerical analysis; Vertical channel; Moving plate

1. Introduction

Mixed convection due to moving surfaces is very important in a wide variety of materials processing systems, such as soldering, welding, extrusion of plastics and other polymeric materials, hot rolling, cooling and/or drying of paper and textiles, chemical vapor deposition (CVD), composite materials manufacturing, as reviewed in [1].

The larger part of research activity on mixed convection with continuously moving vertical surfaces in a quiescent fluid has been developed for a single moving plate, as recently shown in [1,2]. It is recognized that the first studies on a continuously moving sheet were carried out analytically by Sakiadis [3,4]. Detailed theoretical and experimental investigations on the corresponding heat transfer problem were accomplished in [5,6].

The buoyancy force can significantly affect the fluid flow along a vertical moving surface and the first studies on this topic were reported in [6]. This investigation confirmed that flow field and heat transfer from the surface significantly depended on thermal buoyancy force, particularly for low moving surface velocities and large temperature differences between the surface and the ambient fluid.

A boundary layer analysis for laminar mixed convection on an isothermal vertical moving surface in assisting or opposing free stream was carried out in [7]. Correlations of heat transfer rate for a very large range of Prandtl number (10^{-2}–10^4) were presented in all mixed convection domain. Laminar mixed convection in boundary layers adjacent to a vertical, continuously stretching, sheet was analyzed in [8]. Results for the local Nusselt number, the local friction coefficient and temperature profiles were pre-

* Corresponding author. Tel.: +39 081 7682302; fax: +39 081 2390364.
E-mail address: vinaso@unina.it (V. Naso).

0017-9310/$ - see front matter © 2008 Elsevier Ltd. All rights reserved.
doi:10.1016/j.ijheatmasstransfer.2007.11.057

Nomenclature

a	thermal diffusivity, m^2/s
b	channel spacing, m
g	acceleration due to the gravity, m/s^2
Gr	Grashof number, Eq. (1)
h	average convective coefficient, W/m^2 K
k	kinetic energy of turbulence, m^2/s^2
k_f	fluid thermal conductivity, W/m K
L	heated plate length, m
Nu	Nusselt number, Eq. (2)
Pr	Prandtl number, Eq. (1)
q	heat flux, W/m^2
Ra	Rayleigh number, Eq. (1)
Re	Reynolds number, Eq. (1)
Ri	Richardson number, Eq. (1)
s	heated plate thickness, m
T	temperature, K
u	axial velocity component, m/s
U	dimensionless axial velocity component, Eq. (1)
V_b	moving plate velocity, m/s
x, y	Cartesian coordinates, m
X	dimensionless Cartesian coordinate, Eq. (1)

Greek symbols

β	coefficient of thermal expansion, 1/K
ε	dissipation rate of turbulent kinetic energy, m^2/s^3
ν	kinematic viscosity, m^2/s
θ	dimensionless temperature, Eq. (1)

Subscripts

0	ambient
b	belt (moving plate)
c	convective
f	fluid
fc	forced convection
nc	natural convection
p	heated plate
w	wall
x, y	along x or y, respectively

sented. A numerical study of the flow and heat transfer on a continuously stretching surface cooled by a mixed convection flow was carried out in [9]. The effect of buoyancy forces on the flow and heat transfer over a moving heated vertical or inclined surface in an ambient fluid was studied in [10]. The surface moved at a non-uniform velocity and both the constant wall temperature and constant heat flux conditions were considered.

The steady laminar mixed flow and the heat convection on a continuously moving vertical extruded sheet close to and far downstream of the extrusion slot were investigated in [2]. The velocity and temperature variations, obtained by a finite volume method, were used to map out the entire forced, mixed and natural convection regimes.

Mixed convection as a result of buoyancy and motion of one of the channel walls has received little research attention and few guidelines are available for choosing the best performing channel configuration. A study on this topic is presented in [11], where the conjugate mixed convection and conduction heat transfer due to a continuous moving plate in a parallel channel flow was numerically investigated. Results showed that the effect of thermal buoyancy was stronger when the plate moved vertically than when it moved horizontally. The plate velocity affected the overall heat transfer significantly.

It seems that in the open literature there is a lack of information on mixed convection in parallel plate channels with a continuous moving plate in spite of its importance in heat treatment processes.

In the present study a numerical investigation of mixed convection in air due to the interaction between the buoyancy flow and the forced flow induced by a moving plate placed in the mid-plane of a vertical channel is carried out. The moving plate is adiabatic and it moves at a constant velocity in the buoyancy force direction whereas the principal walls of the channel are heated at a uniform heat flux. The problem is numerically solved by means of a finite volume method, using the Fluent code by employing the RNG k–ε model for turbulence with enhanced wall treatment. The effects of channel aspect ratio, Rayleigh and Reynolds numbers are investigated and results in terms of the dimensionless channel wall and moving plate temperatures are given. A composite correlation for Nusselt number in terms of Reynolds and Richardson numbers is proposed in the range from natural convection to forced convection up to $Re = 1.32 \times 10^4$ and $9.86 \times 10^{-6} \leqslant Ri \leqslant 1.15 \times 10^3$, for the channel aspect ratio, $L/(b/2)$, in the [20.3–81.2] range.

2. Mathematical description and numerical procedure

The investigated system is sketched in Fig. 1a. It consists of a vertical channel with a moving plate placed in its mid-plane. The moving plate, in the following also called "belt", moves at a constant velocity in the buoyancy force direction. Both channel walls are conductive and heated at a uniform heat flux, q_w, and their thickness is s. The moving plate is adiabatic and it is assumed to be zero in thickness. The height of the channel is L and its spacing is b. The working fluid is air. Mixed convective flow in the vertical channel is assumed to be incompressible. Moreover, the system is assumed to be wide enough along the third

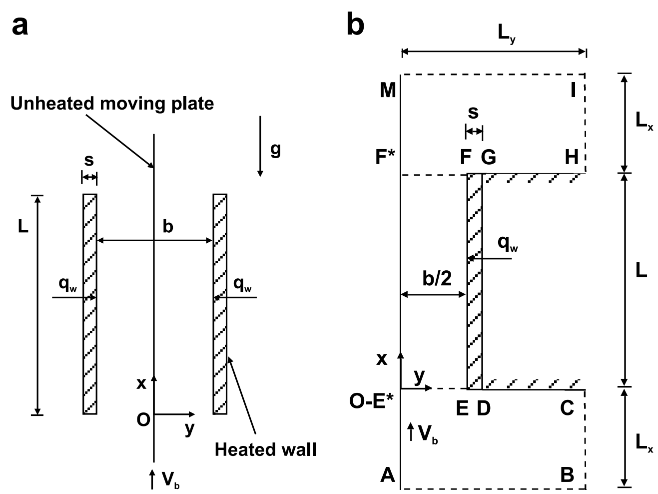

Fig. 1. Sketch of the system: (a) physical domain; (b) computational domain.

coordinate to allow a 2D approximation. All thermophysical properties of the fluid are assumed to be constant, except for the dependence of density on the temperature (Boussinesq approximation). The thermophysical properties of the fluid are evaluated at the ambient temperature, T_0, which is assumed to be 300 K in all cases.

The governing equations for the fluid region in steady state and turbulent regime are time-averaged mass, Navier–Stokes and energy equations [12]. A two-dimensional conduction model in the heated walls is employed whereas the transport equations for k and ε are formulated using the RNG k–ε model.

The dimensionless parameters used in the paper are

$$X = \frac{x}{b/2}; \quad U = \frac{u}{V_b}; \quad \theta = \frac{T - T_0}{q_w(b/2)/k_f}; \quad Re = \frac{V_b b/2}{\nu}; \quad Gr_c = \frac{g\beta q_c (b/2)^4}{k_f \nu^2}; \quad Gr_w = \frac{g\beta q_w (b/2)^4}{k_f \nu^2}; \quad Pr = \frac{\nu}{a}; \quad Ra_c = Gr_c Pr; \quad Ra_w = Gr_w Pr; \quad Ri = Gr_c/Re^2 \tag{1}$$

where q_c is the average convective heat flux, that is the difference between the imposed wall heat flux and the conductive heat flux in the walls.

The average Nusselt number is defined as

$$Nu = \frac{h(b/2)}{k_f} = \frac{q_c}{\overline{T_{w,p}} - T_0}\frac{b/2}{k_f} \tag{2}$$

where $\overline{T_{w,p}}$ is the average heated plate temperature.

An enlarged computational domain has been chosen. It is made up of the vertical channel and of two reservoirs of height L_x and width $2L_y$, downstream and upstream of it, that simulate the free-stream conditions of the flow far away the region thermally disturbed by the heated channel walls. The moving plate extends from the lower to the upper reservoir and its height is $L_b = L + 2L_x$. Thanks to thermofluidynamic and geometrical symmetries, in solving the problem reference was made to half the domain, as shown in Fig. 1b. The imposed boundary conditions are:

- uniform heat flux and no-slip condition on the channel plate EF;
- adiabatic wall and $U = 1$ on the moving plate;
- continuity of the heat flux on the surfaces DE, EF, FG;
- adiabatic wall and no-slip condition on the other solid walls;
- pressure inlet or pressure outlet conditions on the open-boundaries.

The commercial Fluent CFD code was employed to solve the governing equations. The SIMPLE scheme was chosen to couple pressure and velocity. The converging criteria were 10^{-5} for the residuals of the velocity components and 10^{-6} for the residuals of the energy.

Preliminary results showed that the chosen turbulent model (RNG k–ε) was suitable also for laminar flow. Moreover, the RNG k–ε was chosen because it provides an analytically-derived differential formula for effective viscosity that accounts for low-Reynolds-number effects. The enhanced wall treatment approach was employed since it is the most adequate when low-Reynolds-number affects the whole flow domain and for buoyancy-driven flows [13]. Several preliminary tests were carried out to take into appropriate account the effects of turbulence parameters, k and ε, at the inlet. Assuming that the fluid comes from a quiescent zone, the distributions of k and ε were taken

Table 1
Number of subdivisions of the computational domain for three different meshes

Line	Subdivision law	Mesh 1	Mesh 2	Mesh 3
CD	Exponential	75	150	300
AE^*	Uniform	200	400	800
E^*F^*	Uniform	203	406	812
EE^*	Uniform	10	20	40
DE	Uniform	3	6	12

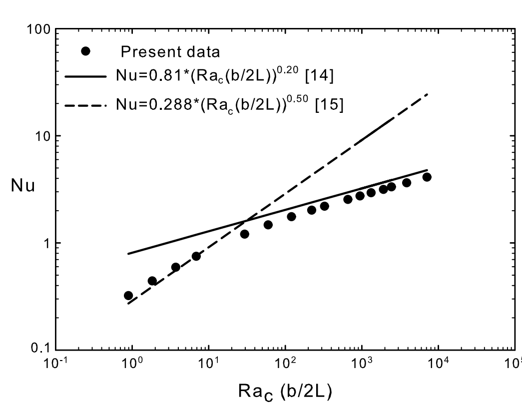

Fig. 2. Comparison between present numerical average Nusselt numbers with correlations given in [14,15], for $V_b = 0$ m/s.

as uniform and equal to 10^{-6}. Moreover, the static pressure upstream and downstream of the channel is set equal to the ambient pressure far away the region of the thermal disturbance induced by the heated channel walls.

As suggested in [13], in order to satisfy the enhanced wall function treatment, different grid sizes were employed for the analysis of the grid independence of the numerical solution. The domain discretization was performed on such a way as to get enough nodes in the channel, where the highest temperature gradients were expected. Moreover, grid independence analysis of turbulent flow simulations is affected by an extra parameter y^+, which is not known a priori. Then numerical experiments are required to reach at the right grid size. A different subdivision along the sides indicated in Fig. 1b was employed. Moreover, a different discretization law was used in the channel region and reservoir regions, as reported in Table 1. A uniform grid was employed along the sides AE*, E*F*, EE* and DE, whereas along CD an exponential law was used. In this case the subinterval length decreased toward the moving plate. Preliminary tests were carried out to evaluate the dependence of the solution on the employed grid. The number of subdivisions for the three meshes employed during the tests is reported in Table 1. A comparison between the average Nusselt number along the heated plate was obtained for $Re = 0$, $Ra = 1.31 \times 10^2$ and $L/(b/2) = 40.6$. The average Nusselt number was 0.673 for Mesh 1, 0.629 for Mesh 2 and 0.611 for Mesh 3. The difference between the values of the average Nusselt number for Mesh 2 and Mesh 3 was about 3%. Mesh 2 was used to obtain the results presented in this analysis because it ensured a good compromise between computational time and accuracy.

A similar analysis has been carried out to set the optimal reservoirs dimensions, L_x and $2L_y$. A common value, equal to 0.400 m, was chosen for L_x and L_y dimensions.

A comparison between the present numerical average Nusselt number values and correlations given in [14,15], for $V_b = 0$ m/s, is shown in Fig. 2. The correlations are, respectively:

$$Nu = 0.81 \times \left(Ra_c\left(\frac{b}{2L}\right)\right)^{0.20} \tag{3}$$

for large values of Rayleigh number $(Ra_c(b/2L) > 2.0 \times 10^3)$ and

$$Nu = 0.288 \times \left(Ra_c\left(\frac{b}{2L}\right)\right)^{0.50} \tag{4}$$

for small values of Rayleigh number, i.e. the fully developed flow.

There is good agreement between numerical data and the two correlations.

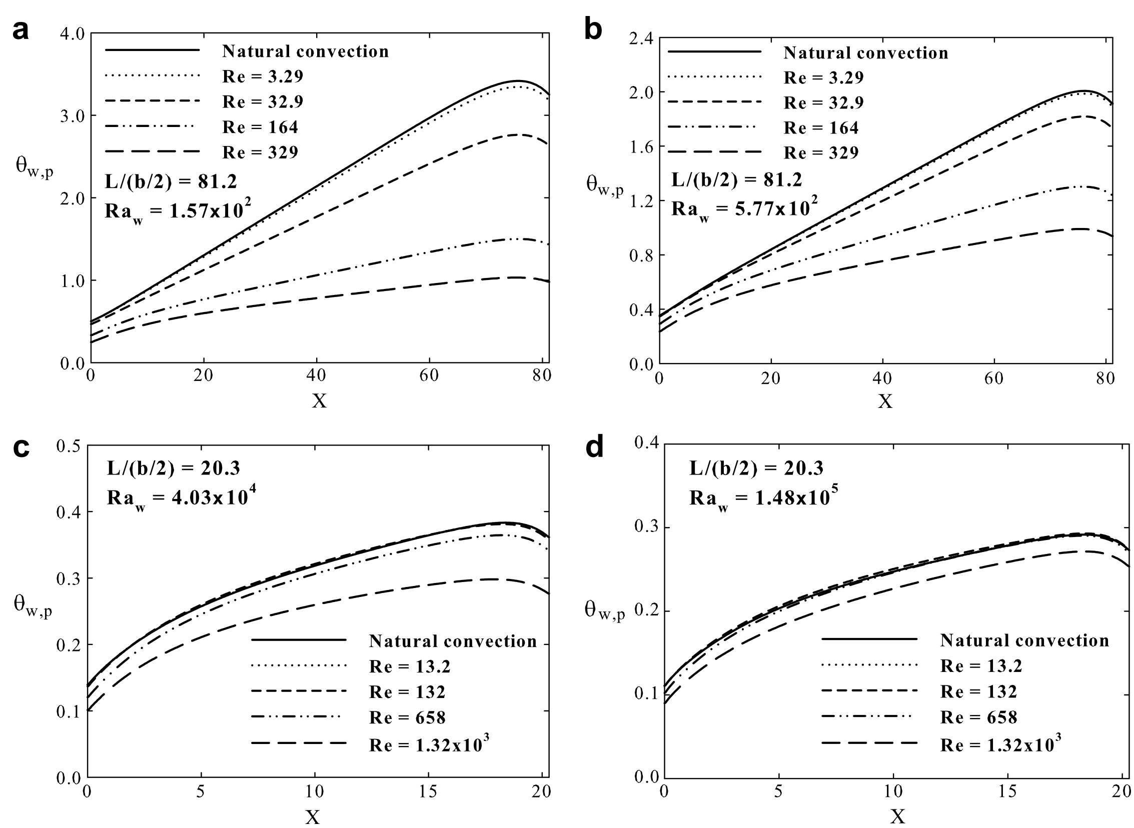

Fig. 3. Dimensionless heated wall temperature vs axial coordinate for natural convection and different Reynolds numbers: (a) $Ra_w = 1.57 \times 10^2$ and $L/(b/2) = 81.2$; (b) $Ra_w = 5.77 \times 10^2$ and $L/(b/2) = 81.2$; (c) $Ra_w = 4.03 \times 10^4$ and $L/(b/2) = 20.3$; (d) $Ra_w = 1.48 \times 10^5$ and $L/(b/2) = 20.3$.

3. Results and discussion

In the following numerical results are presented for $Pr = 0.71$ (air), for a channel aspect ratio $L/(b/2) = 20.3$, 24.6, 40.6 and 81.2 and a Rayleigh number value based on the wall heat flux Ra_w in the range $[1.57 \times 10^2$–$1.48 \times 10^5]$. Computations have been made for natural convection and a Reynolds number value in the range $[3.29$–$1.32 \times 10^4]$. The dimensionless heated plate thickness is $s/(b/2) = 0.16$, 0.19, 0.32 and 0.64.

The dimensionless temperature of the channel walls as a function of the dimensionless axial coordinate X, for the configuration with motionless belt and different values of Reynolds and Rayleigh numbers based on the wall heat flux, is presented in Fig. 3, for $L/(b/2) = 81.2$ and $L/(b/2) = 20.3$.

Fig. 3a shows that when the belt is motionless, that is only natural convection occurs, the dimensionless wall temperature at the channel inlet section ($X = 0$) is not equal to zero because of the fluid preheating in the lower reservoir. In the channel the dimensionless wall temperature increases almost linearly since the flow is nearly fully developed for $L/(b/2) = 81.2$ and $Ra_w = 1.57 \times 10^2$. Due to the edge effects the maximum wall temperature shifts inside the channel and it is attained at a section close to the channel outlet. When the adiabatic plate moves, the heated walls temperature decreases, the higher the Reynolds number the stronger the wall temperature decrease, and the section where the maximum temperature is attained shifts towards the outlet section. For $Re = 164$ and $Re = 329$, the dimensionless wall temperature increase from the entrance to the exit of the channel is far smaller than at lower Reynolds numbers.

Fig. 3b shows that, increasing the Rayleigh number, all other quantities being the same, the dimensionless wall temperature increases. The flow is slightly less developed than in the previous case ($Ra_w = 1.57 \times 10^2$) because of the larger Rayleigh number and the consequent decrease in the boundary layer thickness. The sections where the maximum wall temperature is attained are practically the same as in the previous case. In Fig. 3a, one can notice a decrease in the dimensionless wall temperature slope starting from $X = 5.0$ when the Reynolds number is equal to 164 and 329, because of the interaction between the forced flow induced by the moving plate and the boundary layer adjacent to the channel walls. Fig. 3b points out that Rayleigh number value shifts this starting point to $X \sim 8.0$ since the boundary layer adjacent to the channel wall is thinner. So, comparing the dimensionless wall temperature profiles for the two analyzed Rayleigh number values, one can remark that the flow field is less developed for the larger Reynolds number values. In fact, these profiles show a different slope at the channel inlet section.

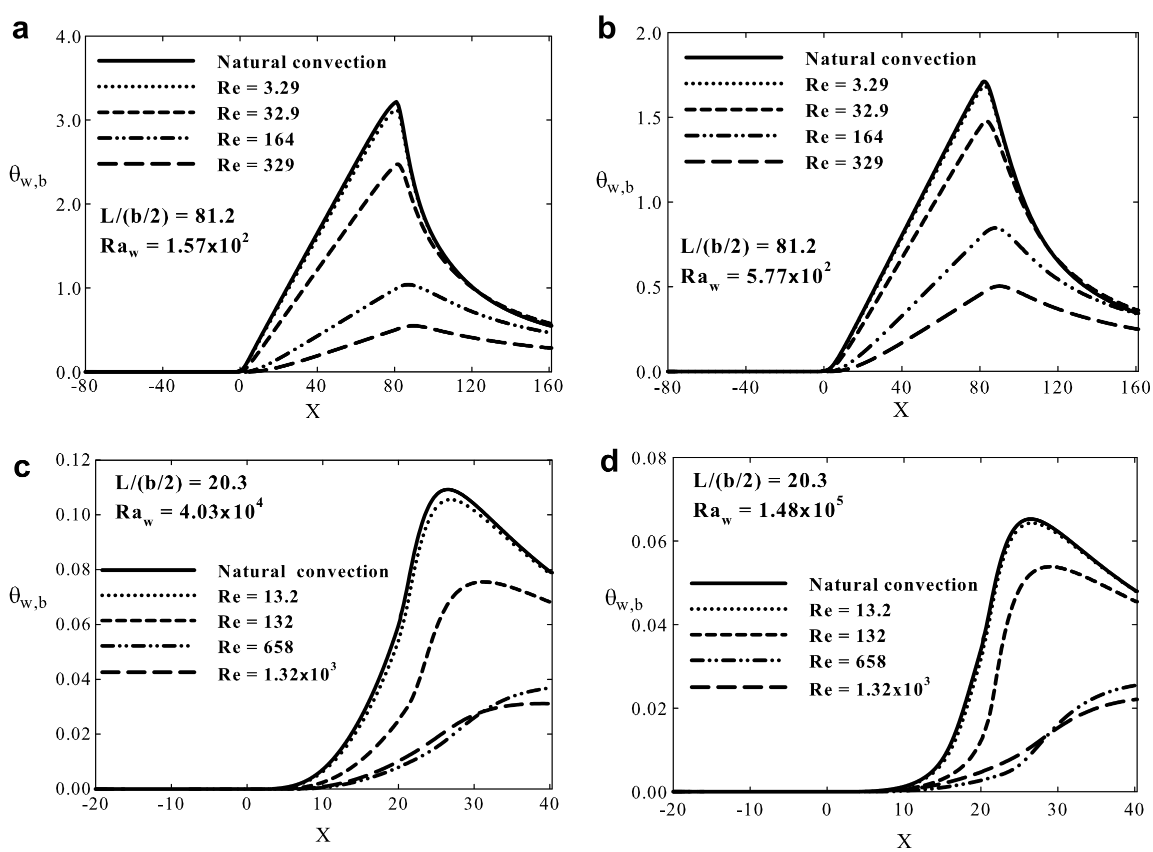

Fig. 4. Dimensionless belt temperature vs axial coordinate for natural convection and different Reynolds numbers: (a) $Ra_w = 1.57 \times 10^2$ and $L/(b/2) = 81.2$; (b) $Ra_w = 5.77 \times 10^2$ and $L/(b/2) = 81.2$; (c) $Ra_w = 4.03 \times 10^4$ and $L/(b/2) = 20.3$; (d) $Ra_w = 1.48 \times 10^5$ and $L/(b/2) = 20.3$.

Fig. 3c and d shows that, decreasing the channel aspect ratio $L/(b/2)$, the dimensionless wall temperature decreases and a less developed flow is exhibited. In comparison with the configuration with a larger aspect ratio, the slope of all temperature profiles is lower for natural convection, $Re = 13.2$ and $Re = 132$, whereas it is larger for $Re = 658$ and $Re = 1.32 \times 10^3$.

The dimensionless temperature of the moving adiabatic plate, as a function of the axial coordinate X, for different values of the Reynolds and Rayleigh numbers and for a channel aspect ratio equal to 81.2 and 20.3 is reported in Fig. 4. Fig. 4a and b shows that in natural convection the thermal disturbance induced by the channel plate does not affect significantly the dimensionless belt temperature upstream of the heated channel inlet, also for $L/(b/2) = 81.2$. Moreover, the dimensionless belt temperature slope is almost constant up to the channel outlet section for both the analyzed Rayleigh number values and for all Reynolds number values. The maximum belt temperature is attained very close to the channel outlet section. Fig. 4b points out that dimensionless temperature profiles are steeper than in Fig. 4a and that the section where the maximum belt temperature is attained shifts toward the end of the channel. When the adiabatic belt is moving, the fluid heated by the channel walls is dragged in the longitudinal direction due to both belt motion and natural convection. The aforementioned fluid drag, for the same Rayleigh number and for larger Reynolds numbers, shifts the maximum belt temperature towards a larger X value, at both investigated channel aspect ratios. For $Re = 329$ and for the two analyzed Ra_w values, the location at which the maximum belt temperature is attained shifts downstream of the channel outlet section, as observed in Fig. 4a and b.

Fig. 4c and d points out that decreasing the channel aspect ratio the section where the maximum belt temperature is attained shifts significantly up, for all Re values. Moreover, at the same Ra_w value, the maximum belt temperature in mixed convection is attained in a farther downstream section than in natural convection. It is worth noticing in Fig. 4c and d that the belt heating starts downstream of the channel inlet section due to the smaller channel aspect ratio and, consequently, to the larger distance between the heated channel walls and the adiabatic plate. This effect is stronger at the larger analyzed Rayleigh number because of the thinner thermal boundary layer adjacent to the heated channel walls. The belt temperatures for $Re = 1.32 \times 10^3$ are higher than those for $Re = 658$ up to $X = 30$, particularly for $L/(b/2) = 20.3$ and $Ra_w = 1.48 \times 10^5$, because of the stronger drag by the moving plate for $Re = 1.32 \times 10^3$, that entrains a larger heated mass flow rate toward the moving plate.

In the following correlations among Nusselt, Reynolds, Grashof based on the convective heat flux and Richardson numbers are presented. The following correlation between Nu and Re when forced convection is prevailing was found by means of the least square method:

$$Nu_{fc} = 0.024 Re^{0.68} \tag{5}$$

with $r^2 = 0.994$, for $Ri < 1.0 \times 10^{-3}$, $3.2 \times 10^2 < Re < 1.32 \times 10^4$.

When only natural convection occurs, the following correlation is proposed:

$$Nu_{nc} = 0.082 Gr_c^{0.34} \tag{6}$$

with $r^2 = 0.978$, for $1.0 \times 10^2 < Gr_c < 2.2 \times 10^5$. All numerical data, in terms of $Nu/Re^{0.68}$ as a function of Ri, are presented in Fig. 5a. The $Nu/Re^{0.68}$ parameter was chosen as the one that yields a good correlation among data. For the sake of comparison, the profiles corresponding to the correlations in Eqs. (5) and (6) are also reported in Fig. 5a. The term $Nu/Re^{0.68}$ as a function of Richardson number shows that Nusselt numbers for $Ri < 2.0 \times 10^{-3}$ are in good agreement with the correlation (5) and for $Ri > 10^{-1}$ the Nusselt numbers are in good agreement with the correlation (6) for natural convection. All numerical data are correlated, combining Eqs. (5) and (6), by the equation:

$$\frac{Nu}{Re^{0.68}} = \left[\left(\frac{Nu_{nc}}{Re^{0.68}}\right)^{3.5} + \left(\frac{Nu_{fc}}{Re^{0.68}}\right)^{3.5}\right]^{(1/3.5)} \tag{7}$$

with $r^2 = 0.967$, in the range $9.86 \times 10^{-6} < Ri < 1.15 \times 10^3$. The composite correlation and numerical data are presented in Fig. 5b, that points out a very good agreement between them.

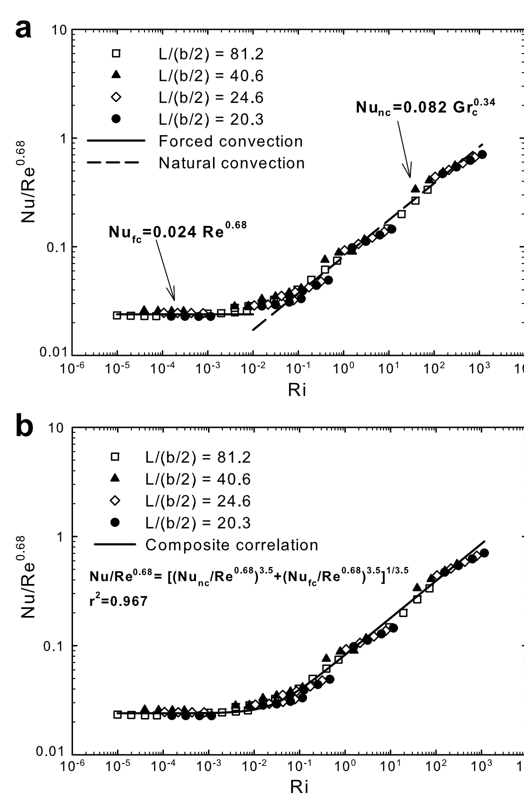

Fig. 5. Comparison among all numerical data in terms of $Nu/Re^{0.68}$ as a function of Richardson number and: (a) the two correlations in dominated forced and natural convection regimes; (b) the composite correlation (7).

4. Conclusions

The numerical investigation of mixed convection in air due to the interaction between a buoyancy flow and a forced flow induced by an adiabatic moving plate located in the mid-plane of a vertical channel was carried out. The moving plate moved at a constant velocity in the buoyancy force direction and the principal walls of the channel were heated at uniform heat flux.

The numerical analysis showed that for the lowest analyzed Rayleigh numbers based on the wall heat flux, dimensionless wall temperatures decreased significantly when the Reynolds number increased. At increasing Reynolds number the flow field was less developed. For the lowest channel aspect ratio, $L/(b/2) = 20.3$, the effect of the moving plate was not strong even at the larger Reynolds number, $Re = 1.32 \times 10^3$, and the lower the Rayleigh number the weaker the effect of the Reynolds number.

The maximum temperature of the moving plate was attained as far from the channel outlet section as the lower the channel aspect ratio was. For the lower analyzed channel aspect ratio, natural convection due to the heated plate was less influent than the forced flow induced by the moving plate.

A composite correlation to evaluate the average Nusselt number in terms of Richardson and Reynolds numbers in the range $9.86 \times 10^{-6} \leqslant Ri \leqslant 1.15 \times 10^3$, for $20.3 \leqslant L/(b/2) \leqslant 81.2$ from natural convection to forced convection up to $Re = 1.32 \times 10^4$, was proposed. Numerical data and the composite correlation were compared and they showed a very good agreement.

Acknowledgement

This work was supported by MIUR with a 2005 PRIN grant.

References

[1] Y. Jaluria, Thermal processing of materials: from basic research to engineering, J. Heat Transfer 125 (6) (2003) 957–979.
[2] S.A. Al-Sanea, Convection regimes and heat transfer characteristics along a continuously moving heated vertical plate, Int. J. Heat Fluid Flow 24 (2003) 888–901.
[3] B.C. Sakiadis, Boundary-layer behaviour on continuous solid surfaces: I. Boundary-layer equations for two-dimensional and axisymmetric flow, AIChE J. 7 (1961) 26–28.
[4] B.C. Sakiadis, Boundary-layer behaviour on continuous solid surfaces: II. The boundary-layer on a continuous flat surface, AIChE J. 7 (1961) 221–225.
[5] F.K. Tsou, E.M. Sparrow, R.J. Goldstein, Flow and heat transfer in the boundary layer on a continuous moving surface, Int. J. Heat Mass Transfer 10 (2) (1967) 219–235.
[6] A. Moutsoglou, T.S. Chen, Buoyancy effects in boundary layers on inclined, continuous, moving sheets, J. Heat Transfer 102 (1980) 371–372.
[7] H.T. Lin, H.L. Hoh, Mixed convection from an isothermal vertical flat plate moving in parallel or reversely to a free stream, Heat Mass Transfer 32 (1997) 441–445.
[8] C.H. Chen, Laminar mixed convection adjacent to vertical, continuously stretching sheets, Heat Mass Transfer 33 (1998) 471–476.
[9] C.H. Chen, Mixed convection cooling of a heated, continuously stretching surface, Heat Mass Transfer 36 (2000) 79–86.
[10] A.J. Chamkha, H.S. Takhar, G. Nath, Effect of buoyancy force on the flow and heat transfer over a continuous moving vertical or inclined surface, Int. J. Therm. Sci. 40 (2000) 825–833.
[11] Y. Jaluria, B.H. Kang, Heat transfer from continuously moving material in channel flow for thermal processing, J. Thermophys. Heat Transfer 8 (3) (1999) 546–554.
[12] M. Rokni, B. Sundén, Turbulent forced convection in ducts, in: B. Sundén, G. Comini (Eds.), Computational Analysis of Convection Heat Transfer, WIT Press, Southampton, UK, 2000, pp. 361–407.
[13] Fluent Incorporated, Fluent 6.2, User Manual, Lebanon, NH, 2005.
[14] O. Manca, S. Nardini, Composite correlations for air natural convection in tilted channels, Heat Transfer Eng. 20 (3) (1999) 64–70.
[15] W. Aung, Fully developed laminar free convection between vertical plates heated asymmetrically, Int. J. Heat Mass Transfer 15 (1972) 1577–1580.